



Rapid fingerprinting of source and environmental microplastics using direct analysis in real time-high resolution mass spectrometry

Xianming Zhang ^{a, **}, Alicia Mell ^a, Frederick Li ^b, Clara Thayesen ^c, Brian Musselman ^b, Joseph Tice ^b, Dragan Vukovic ^d, Chelsea Rochman ^c, Paul A. Helm ^a, Karl J. Jobst ^{a, e, *}

^a Ontario Ministry of the Environment, Conservation and Parks, Toronto, Ontario, M9P 3V6, Canada

^b IonSense Inc. Saugus, Massachusetts, 01906, USA

^c Department of Ecology and Evolutionary Biology, University of Toronto, Toronto, Ontario, M5S 3H6, Canada

^d VBM Science Ltd, Dundas, Ontario, L9H 6Y7, Canada

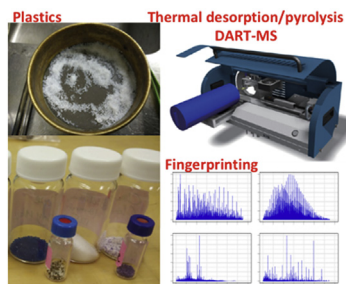
^e Department of Chemistry, Memorial University of Newfoundland, St. John's, NL A1B 3X7, Canada



HIGHLIGHTS

- Microplastics are characterized by Direct Analysis in Real Time-high resolution mass spectrometry.
- Thermal decomposition thereof yields a mixture of products, i.e. the “chemical fingerprint”.
- Chemical fingerprints are compared using multivariate statistics and graphical visualization.
- The approach may be used to determine the identity of microplastics and potentially their sources.
- The method is applied to microplastics from Lake Ontario as well as various personal care products.

GRAPHICAL ABSTRACT



ARTICLE INFO

Article history:

Received 14 August 2019

Received in revised form

29 November 2019

Accepted 1 December 2019

Available online 3 December 2019

Keywords:

Environmental mass spectrometry

Direct Analysis in Real Time

Microplastics

ABSTRACT

Microplastics are ubiquitous in the aquatic and terrestrial environment. To prevent further contamination, methods to determine their sources are needed. Techniques to quantify and characterize microplastics in the environment are still evolving for polymers and the additives and leachable substances embedded therein, which constitute the “chemical fingerprint” of an environmental microplastic. There is a critical need for analytical methods that yield such diagnostic information on environmental microplastics that enables identification of their composition and sources of pollution. This study reports on a novel approach for rapid fingerprinting of environmental microplastics and the screening of additives using Direct Analysis in Real Time (DART)-high resolution mass spectrometry. A variety of plastic samples were investigated, including virgin pre-production pellets, microbeads from personal care products, microplastics found in the aquatic environment, and synthetic fibers. The resulting mass spectra display ~10,000 discrete peaks, corresponding to plastic additives released by thermal desorption

* Corresponding author. Memorial University of Newfoundland, St. John's, NL A1B 3X7, Canada.

** Corresponding author.

E-mail addresses: xianming.zhang@gmail.com (X. Zhang), li@ionsense.com (F. Li), clara.thayesen@utoronto.ca (C. Thayesen), [\(B. Musselman\)](mailto:musselman@ionsense.com), dragan@vbmscience.com (D. Vukovic), chelsea.rochman@utoronto.ca (C. Rochman), paul.helm@ontario.ca (P.A. Helm), [\(K.J. Jobst\)](mailto:kjobst@mun.ca).

High-resolution mass spectrometry
Chemical fingerprinting

and polymer degradation products generated by pyrolysis. These were used to characterize differences among plastic types, microplastic source materials, and environmental samples. Multivariate statistics and elemental composition analysis approaches were applied to analyze fingerprints from the mass spectra. This promising analytical approach is sensitive, (potentially) high-throughput, and can aid in the elucidation of possible sources of microplastics and perhaps eventually to the analysis of bulk environmental samples for plastics.

© 2019 Elsevier B.V. All rights reserved.

1. Introduction

Global plastic production has rapidly increased since the 1950s and the current annual production exceeds 300 million tonnes [1]. Of all the plastic that has been produced, nearly 80% ends up in landfills or in the natural environment [2]. Over time, these plastics break down into smaller and smaller pieces called microplastics (plastic particles smaller than 5 mm). Microplastics enter the environment via wastewater, industrial spills, accidental loss from waste management facilities, and through the breakdown of larger pieces of littered plastic [3,4]. Their presence in freshwater and marine ecosystems is now well documented [5–8], and microplastics have thus become an emerging global environmental contaminant.

Concerns of microplastics in the environment arise from ingestion of plastic particles by terrestrial and aquatic life; from physical interactions with the particles (e.g. Refs. [6,9,10]); and from polymer compositions and additives such as plasticizers and flame retardants [11]. For example, monomers from plastics such as polystyrenes and epoxy resins have been identified as mutagenic and carcinogenic [11]. Some plasticizers and flame retardants are known endocrine disruptors [12,13]. Due to these potential hazards, there have been calls to change societal views of how plastic waste is handled and sources are managed [14,15].

Effective assessment and management of risk from microplastic contamination requires detailed information on their sources, which may be characterized using a variety of analytical techniques [16–18]. The morphology of environmental microplastics, visually characterized by microscopy, can help infer sources [19]. For example, perfectly spherical microplastics less than 1 mm in size are likely microbeads from personal care products, whereas particles with a twisted, curved character are likely 'trimmings' or 'flash' from manufacturing and molding processes [19]. Methods to characterize polymeric identity of particles, such as Raman and Fourier transform infrared (FTIR) spectroscopy [20] can also be used to infer sources because plastic of a specific polymer type is more commonly used in certain sectors than others. For example, polyethylene is mostly used in packaging applications, while PVC is primarily used in the building and construction sector [2].

Microscopy and Raman and FTIR spectroscopy have their advantages, but both often require laborious, particle-by-particle characterization. Visual characterization also requires subjective judgment from the analyst, and spectroscopic characterization is subject to interference by dyes, process aids, and metals present in plastics, which can result in false positives and negatives in identifying polymers [20–22]. While recently developed spectroscopy-based imaging techniques enable better characterization and fingerprinting of microplastics [23], the visual techniques are not amenable to the analysis of additives present at part-per-million concentrations since detection limits via FTIR and Raman spectroscopy are still high for minor chemical constituents.

Mass spectrometry (MS) coupled with gas chromatography (GC), is an alternative approach that has attracted recent attention

for qualitative and quantitative analysis of microplastics. This approach relies upon thermal desorption or pyrolysis to introduce additive chemicals and thermally decomposed products from the polymers to the GC-MS [24–29]. The total ion chromatogram, referred to as a pyrogram when a pyrolysis inlet is used [24], reflects the polymer degradation products as well as additives and leachable substances, which constitute the "chemical fingerprint" of an environmental microplastic [24]. Fries et al. [24] suggest that this approach could potentially be used to identify sources of microplastic pollution on the basis of their chemical fingerprint.

There are some limitations imposed by using GC with low-resolution quadrupole mass spectrometry. First, the complex mixture generated from pyrolysis needs to be separated by GC, which in turn limits the throughput of analysis and reduces the number of higher molecular weight compounds that can be included in the chemical fingerprint. Such separation normally requires 30–60 min, and thus cannot be considered "rapid". Second, the complexity of the pyrolysis mixture is comparable to that of crude oil [30] and cannot be separated using gas chromatography, unless multidimensional separation is performed (Byer et al., 2016; Bowman et al., 2019). In contrast, high resolution mass spectrometry (HRMS) is capable of accurately determining thousands of unique elemental compositions, which represent a more detailed fingerprint than what can be obtained using GC-MS and may well enable differentiation of subgroups (and sources) of microplastics of the same polymer type.

Ambient ionization techniques such as Direct Analysis in Real Time (DART) [31,32] have been increasingly used for rapid characterization of polymers with little, if any, sample preparation. This technique may well enable rapid characterization and source-apportionment of environmental microplastics, but to our knowledge, a method has not been reported until now. In this study, we investigate thermal desorption and pyrolysis with DART for high resolution characterization of source polymers and environmental microplastics. The high-resolution mass spectra obtained from thermal desorption and pyrolysis experiments were analyzed to produce chemical fingerprints inclusive of additives and thermal decomposition products to help characterize and classify microplastics by polymer and within similar polymer types.

2. Materials and methods

2.1. Samples of polymers and environmental microplastics

This study reports on the analysis of 21 plastic samples, including plastic pellets from polymer manufacturers, microbeads from personal care products, microplastics collected from the aquatic environment, and synthetic fibers (Table 1). Four pre-production pellet plastics, including low-density polyethylene (LDPE), polypropylene (PP), high impact polystyrene (HIPS), and polyethylene terephthalate (PET), were ground to particles of 0.3–1 mm in size. These were either analyzed directly or treated via wet peroxidation (WPO), as is often done for environmental

Table 1

Sample information for microplastic particles included in this study.

#	Name	Description
01	LDPE	Low density polyethylene ground plastic pellets; 0.3–1 mm
02	Digested LDPE	Wet peroxidation (WPO) digested ground LDPE
03	PP	Polypropylene ground plastic pellets; 0.3–1 mm
04	Digested PP	Wet peroxidation (WPO) digested ground PP
05	HIPS	High impact ground polystyrene plastic pellets; 0.3–1 mm
06	Digested HIPS	Wet peroxidation (WPO) digested ground HIPS
07	PET	Polyethylene terephthalate ground plastic pellets; 0.3–1 mm
08	Digested PET	Wet peroxidation (WPO) digested ground PET
09	LDPE/PET/HIPS Mix	Equal mass mix of ground LDPE, PET, and HIPS particles
10	Face Wash A; White	Exfoliating scrub; white polyethylene microbeads
11	Face Wash A; Purple	Exfoliating scrub; purple cera microcrystalline microbeads
12	Body Wash A	Body Wash; White microbeads
13	Face Wash B	Exfoliating face wash; white polyethylene microbeads
14	Body Wash B	Body Wash; White microbeads
15	Toronto Harbor	Mix of particles (0.3–1 mm) from manta trawl, collected from Toronto Harbor, Lake Ontario; WPO digested
16	Humber Bay	Mix of particles (0.3–1 mm) from manta trawl, collected from Humber Bay, Lake Ontario; WPO digested
17	West Basin Lake Erie	Mix of particles (0.3–1 mm) from manta trawl, collected from western basin, Lake Erie; WPO digested
18	Polyester Fleece Yellow	Consumer fabric: yellow polyester (100%) fleece fibers
19	Polyester Fiber Red	Consumer fabric: red polyester (100%) fibers
20	Nylon Fiber Red	Consumer fabric: red nylon (100%) fibers
21	Nylon Spandex Yellow	Consumer fabric: bright yellow nylon (80%) spandex (20%) fibers

samples (described below). An equal-mass mixture of LDPE, PP, and PET was also prepared and analyzed. Samples of microbeads in personal care products were isolated from select retail products via sieving and rinsing with water and ethanol. These products included two exfoliating face scrubs, including two types of beads in one product, and two body washes.

Environmental microplastics were collected by manta trawls from two locations in Lake Ontario adjacent to the large urban center of Toronto, Ontario, Canada (Toronto Harbor, Humber Bay) and the west basin of Lake Erie downstream of Windsor, Ontario, Canada and Detroit, Michigan, USA. Plastic particles were isolated from the bulk samples by WPO digestion using $\text{Fe}^{2+}(0.5 \text{ M})/\text{H}_2\text{O}_2$ (30%) at up to 60 °C [33]. A variety of particles from the 0.3–1 mm size fraction were combined for analysis. Polymeric fibers of different colours were obtained from a consumer fabric store and included two polyester materials and two nylon-containing materials (Table 1).

2.2. Instrumental analysis

Sample analysis was performed using a Q Exactive hybrid quadrupole-orbitrap mass spectrometer (ThermoFisher Scientific, Bremen, Germany) coupled to a Direct analysis in real time (DART) ion source (IonSense Inc., Saugus, Massachusetts, USA). The samples were introduced to the mass spectrometer using an IonRocket thermal desorption/pyrolysis inlet (BioChromato Inc., San Diego, California), see Fig. 1A.

Individual samples of the plastic pellets, microbeads or environmental microplastics (~5 mg) were loaded to the IonRocket sample stage (Fig. 1B), which was initially held at ambient temperature, heated to 50 °C over 2 min, ramped to 600 °C over the next 6 min and then held for 2 min at 600 °C. Additive compounds and degradation products released during thermal desorption and pyrolysis were ionized by DART operated in the positive mode using He (5.0 grade) as the reagent gas. The DART grid voltage and heater were set to 350 V and 300 °C respectively. Ionization by DART involves a rich chemistry of gas-phase (ion-molecule) reactions, which is described in the recent review by Gross [34]. Briefly, ionization is initiated by Penning (or chemi-) ionization of ambient gas molecules in the ion source, followed by secondary ion-molecule reactions with analyte molecules (M). For example, the interactions between metastable helium (He^*) and ubiquitous H_2O

molecules leads to the formation of H_2O^{+} ions, which rapidly react with other protic molecules to form reagent ions H_3O^{+} . The predominant ions observed in this study were the proton adducts ($[\text{M}+\text{H}]^+$) of analyte molecules (M), but molecular ions M^{+} and ammonium adducts ($[\text{M} + \text{NH}_4]^+$) may also be generated, depending on the proton affinity of M. The Orbitrap mass spectrometer was operated at a resolution of 70,000 fwhm (full-width half-maximum – at m/z 200) with a scan frequency of 2Hz across a mass range of 50–750 Da.

2.3. Data analysis

Mass spectra were collected over the course of a 10-min sample analysis (Fig. 1C). We selected 2–4 min (phase II; 50–230 °C) and 5.5–7 min (phase IV: 370–510 °C) to characterize additives released from thermal desorption and polymer degradation products generated by pyrolysis, respectively. Using the R package of enviPat (v 2.2) [35], the monoisotopic masses and isotope distributions for a list of 206 common plastic additives were calculated, anticipating that the (quasi)molecular ions $[\text{M}+\text{H}]^+$, $[\text{M}+\text{NH}_4]^+$ and M^{+} would be generated. The suspect list consists of common accelerators, stabilizers, antioxidants, coupling agents, flame retardants, and plasticizers [36].

The predicted masses and isotope distributions were then compared with the mass spectra collected at the thermal desorption stage. Plastic additives in the samples were tentatively identified if mass error was <5 part per million (ppm, calculated as $10^6 \Delta m/m$ and used as a unit for mass error and differences); deviation of the relative abundance of the ^{13}C isotopic peak from theoretical values was less than 15%. Additive compounds that were detected in all samples were ignored as potential background contaminants. Elemental compositions of mass peaks generated at the pyrolysis stage were assigned based on the Seven Golden Rules [37] of organic molecules using the FTMS Visualization package [38]. Elemental limits were set to $\text{C}_{0–60}\text{H}_{0–200}\text{O}_{0–10}\text{N}_{0–2}\text{S}_{0.1}$ with mass error threshold of 5 ppm. Profiles of raw mass spectra and assigned chemical classes (log-transformed and normalized intensities) were analyzed with principal components analysis (PCA) and hierarchical clustering using functions (prcomp, hclust) in the R statistical package (version 3.3.3). Masses that are not detected in a sample were assigned with a random number between 0 and the lowest intensity of mass peaks detected for the statistical analyses.

3. Results and discussion

3.1. Interpreting the high-resolution mass spectra obtained by pyrolysis of plastics

The high-resolution mass spectra (m/z 50–750) obtained by pyrolysis of the microplastic samples are displayed in Fig. 2. At first

glance, identification of the dominant peaks in each mass spectrum is relatively straightforward. The mass spectra obtained by pyrolysis of PE and PP are characterized by series of homologous ions differing by CH_2 unit (14 amu) and C_3H_6 (42 amu) respectively, which result from cleavages all along the backbone of the polymer. Decomposition of HIPS and PET predominantly yields dimers, trimers and the corresponding oxidized products. The most abundant

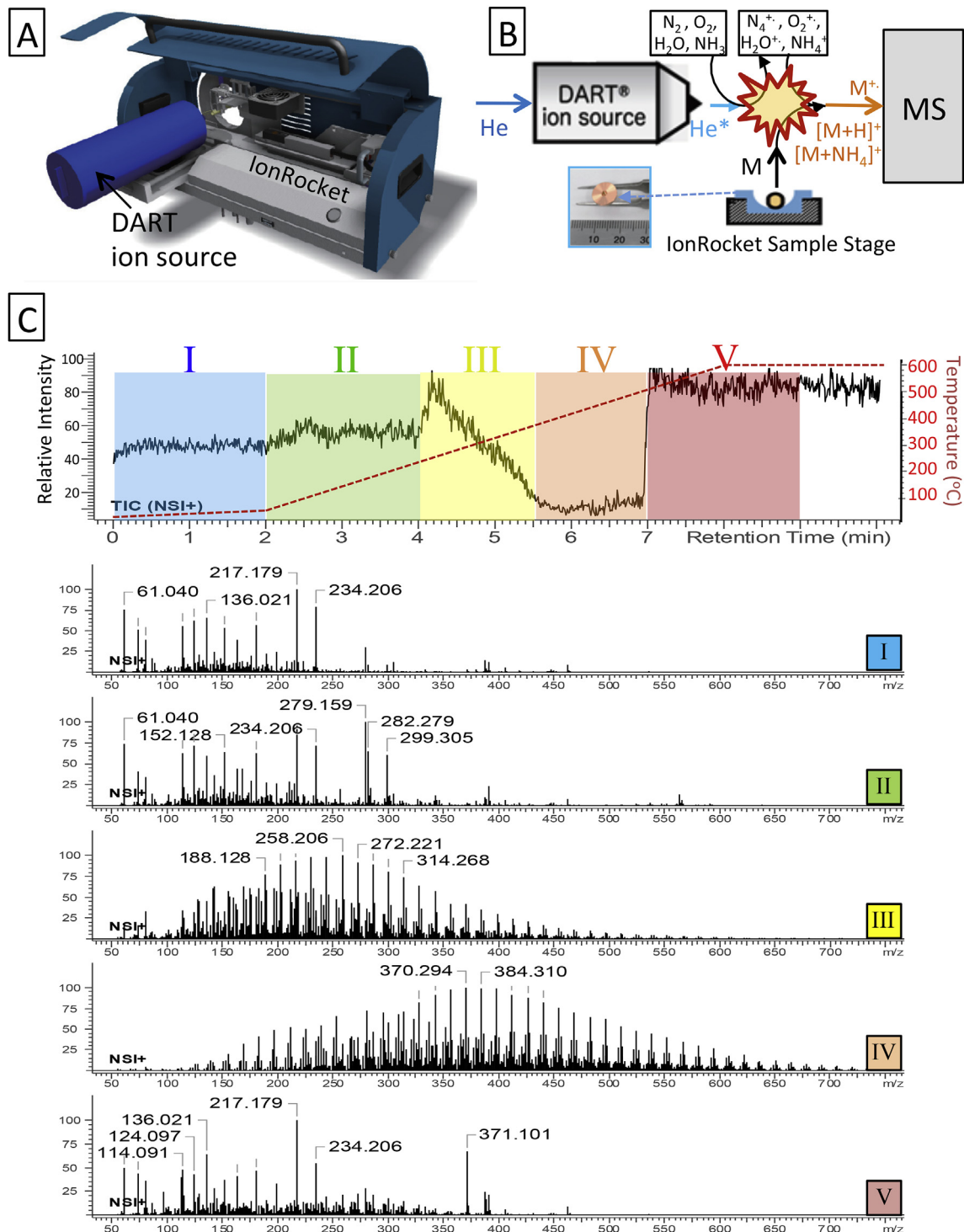


Fig. 1. (A) Schematic and (B) ionization mechanism of the IonRocket thermal desorption/pyrolysis unit coupled with direct analysis in real time (DART) ion source used in this study for plastic characterization. Using untreated polyethylene as an example, Panel C illustrates different mass spectra (I to V of panel C) generated as a sample is heated from ambient temperature to 600 °C, during which thermal desorption of volatile compounds in the polymers and pyrolysis (thermal decomposition) of the polymers occur.

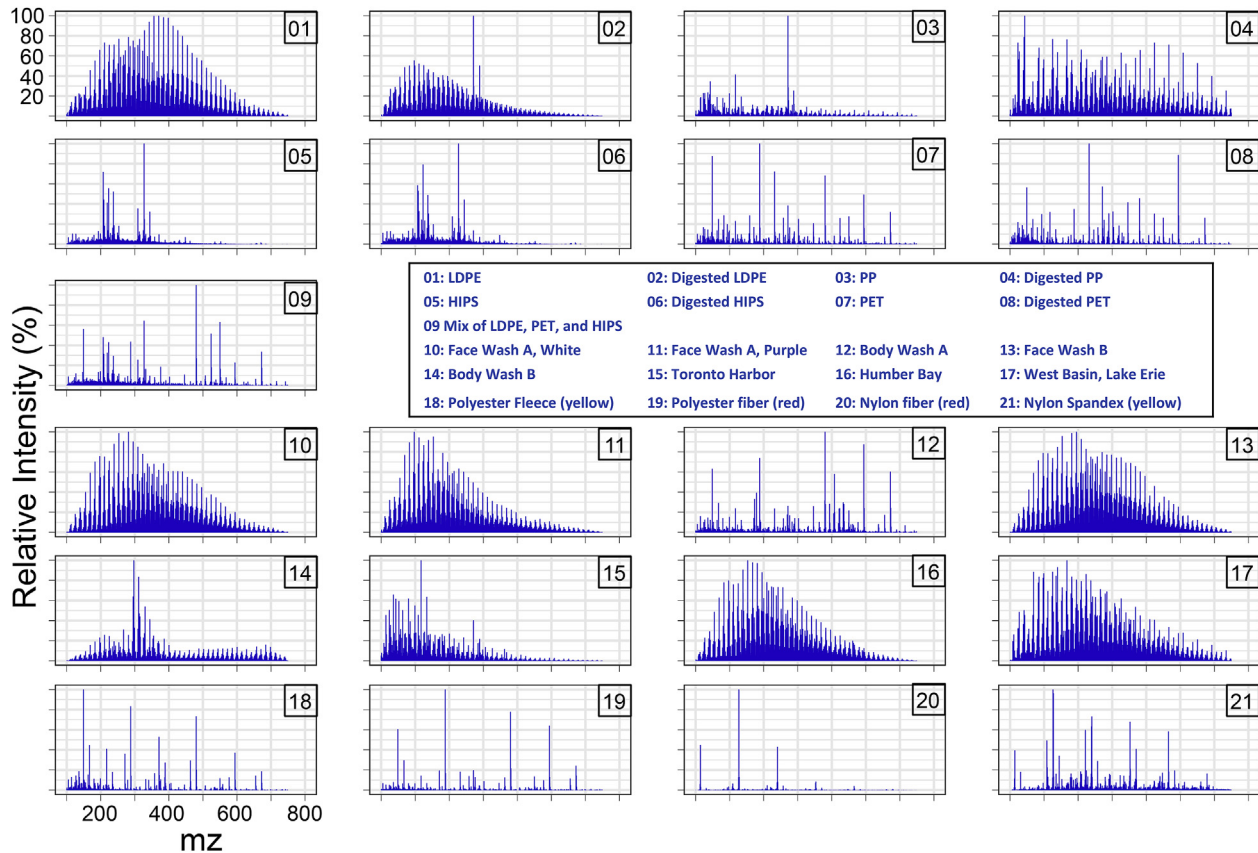


Fig. 2. Mass spectra of complex chemical mixtures generated from pyrolysis of raw plastic materials (01–08), a mixture (09) of low density polyethylene (LDPE), polyethylene terephthalate (PET) and high impact polystyrene (HIPS), microplastics from personal care products (10–14) and from the environment (15–17), and synthetic fibers (18–21).

ions from HIPS include m/z 327.173, 223.111, and 207.116, which correspond to the oxidized trimer ions $[C_{24}H_{22}O + H]^+$ and the dimers $[C_{16}H_{14}O + H]^+$, and $[C_{16}H_{14}+H]^+$ [39]. Montaudo et al. [39] have studied in detail the thermal degradation mechanisms of PET and proposed the formation of both open and cyclic oligomers as the primary products. For example, the mass spectrum of PET (Fig. 2) displays two abundant ions with m/z 594.159 and m/z 149.059 that correspond to the ammoniated cyclic trimer $[C_{30}H_{24}O_{12}+NH_4]^+$ and one of its dissociation products $[C_9H_8O_2+H]^+$. The peak at m/z 332.112 may well be the ammonium adduct of $HOC(=O)-Ph-C(=O)O-(CH_2)_2-O-C(=O)-Ph$, a monomeric ion with elemental composition $[C_{17}H_{14}O_6+NH_4]^+$. Pyrolysis of nylon predominantly leads to the formation of the monomer, dimer, trimer and tetramer ions $[C_6H_{11}NO+H]^+$, $[C_{12}H_{23}N_2O_2+H]^+$, $[C_{18}H_{33}N_3O_3+H]^+$ and $[C_{24}H_{44}N_4O_4+H]^+$, which is consistent with previous chemical ionization experiments [40].

Each mass spectrum consists of over 10,000 discrete peaks, of which approximately 800–3000 (6–20%) contribute to 95% of the total signal intensity. This reflects the complexity of the mixtures of compounds generated by pyrolysis. As illustrated by the decomposition of polyethylene (Fig. 3), within a nominal mass there exist multiple peaks corresponding to elemental compositions that differ by heteroatom content (e.g. the O₃, SO, S₂O, NO₂₋₆ classes are displayed in Fig. 3). Pyrolysis and thermal decomposition undoubtedly involves autooxidation, resulting in the formation of oxygen containing compounds (e.g. the O₃ class), which may also be detected as $[M + NH_4]^+$ adducts [34,41]. While the mass resolution employed in this experiment (c. 70,000 fwhm) is insufficient to resolve the C₃/SH₄ mass split (Byer et al., 2016), we propose that the m/z 371.334 peak in Fig. 3 corresponds to C₂₂H₄₃SO (0.5 ppm) rather

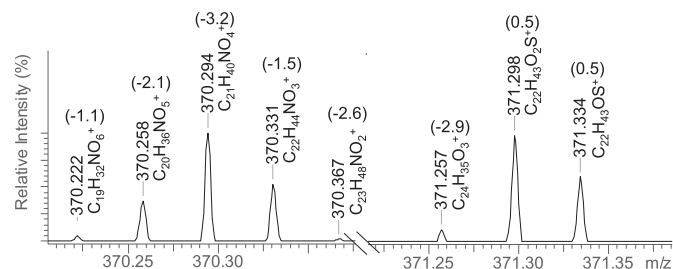


Fig. 3. Partial mass spectra of low-density polyethylene sample around m/z 370 and 372. The spectra display multiple peaks within a narrow (sub amu) mass range. Numbers in parentheses are the differences (ppm) between experimental and theoretical masses.

than C₂₆H₄₃O (8.5 ppm) due to the small deviation between experimental and exact masses. That sulfur-containing species are generated during thermal decomposition suggests the use of sulfur additives to improve the mechanical stability of the plastics [42]. This illustrates our supposition that high resolution measurements provide important polymer composition information that would otherwise be difficult to obtain by other methods.

The mass spectra were analyzed with principal component analysis (Fig. 4). Each principal component represents a group of ions that correlates with one another. With only three principal components, polyolefin (PE and PP, samples 1–4), PS (5 and 6), PET (7 and 8), polyester (18 and 19) and nylon (20 and 21) can be distinguished from each other. It is also gratifying to note that the identities of *unknown* microplastics (samples 10–17) could also be

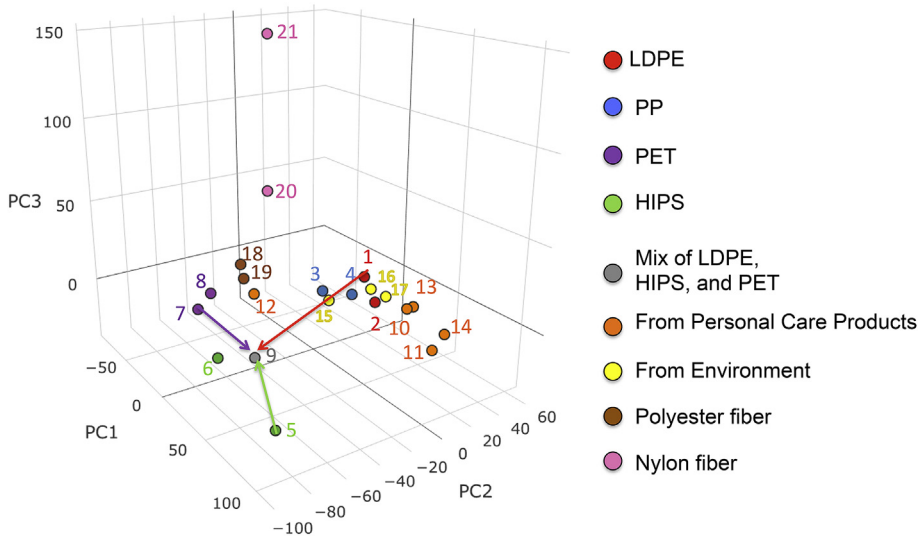


Fig. 4. Principal component analysis of the mass spectra (c. 95% of total intensity) obtained by pyrolysis of the plastic samples. Based on the scores of the first three principal components (PC1-3), polyolefin, polyethylene terephthalate (PET), high impact polystyrene (HIPS) and nylon can be distinguished. The arrows connect the three plastics (1,5,7) used to prepare the mixed sample (9).

inferred based on their position in Fig. 4.

Higher positive scores on PC1 reflect lower abundances of $C_cH_hO_oN$ ions (ammonium adducts) relative to the $C_cH_hO_o$ ions (c, h, o represents the number of carbon, hydrogen and oxygen atoms). The polyolefins are differentiated from the other types of plastic based on the scores of PC2, which correlated with decreased aromatic structures in the polymers and thus lower double bond equivalents (DBE). The two nylon samples had elevated scores of PC3, which is related to the ions that contain multiple nitrogen atoms. Based on the distributions of samples on the PCA plot, we determined that most plastic beads used in personal care products (samples 10, 11, 12, 13) had polyolefinic character, and that the mixed particles from bulk environmental samples (samples 15, 16, 17) were dominated by polyolefins. In contrast, the microbeads from personal care products in sample 12 clustered with PET. The polyester samples (18 and 19) also grouped together with PET. Sample 9 is a mixture of undigested LDPE, HIPS and PET (sample 1, 5, and 7). Consequently, it was located in between the individual samples on the PCA plot, reflecting the mixture of polymer fingerprints. Identifying signature compounds for each plastic is a critical first step towards quantitative analysis of different plastic types. The results presented here suggest that the full mass spectral fingerprint may provide additional target masses to help differentiate, confirm, and quantify some plastics, especially in more complex environmental samples. Other significant challenges associated with microplastics determination have been reviewed recently by Silva et al. [43].

3.2. Chemical class profiles of the pyrolytic and thermal decomposition products

Principal component analysis (Fig. 4) resulted in relatively little separation between polyethylene and polypropylene, despite the fact that their mass spectra (Fig. 1) are characteristically different: the spectra obtained from polyethylene and polypropylene display intense homologous ions that differ by CH_2 (14 amu) and C_3H_6 (42 amu) units respectively. As shown in Fig. 3, there are several homologous series that differ by heteroatom content, and generally display the same carbon number distribution. For example, the O_3 chemical class corresponds to all ions with the elemental

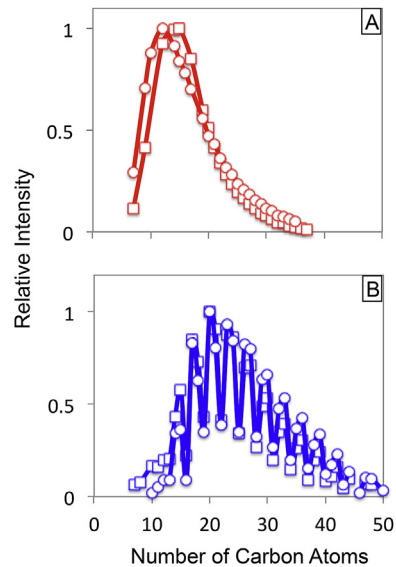


Fig. 5. Carbon number distributions of ions $[C_cH_{2c-6}O_3+H]^+$ generated from pyrolysis of polyethylene (A) and polypropylene (B). Squares: raw samples; Circles: digested samples.

composition $[C_cH_hO_o + H]^+$. The differences between PE and PP become obvious when, see Fig. 5, the distribution of ions $[C_cH_{2c-6}O_3+H]^+$ is graphed as a function of carbon number. Decomposition products with 12–14 carbons are the most abundant in polyethylene whereas the most abundant compounds generated from polypropylene have a carbon number of 20. Comparing raw and digested samples, we find the sample preparation processes do not affect fingerprints based on carbon number distributions.

Chemical classes present in over 50% of the samples were selected and analyzed with hierarchical cluster analysis (HCA), the results of which are summarized by the heat map in Fig. 6. The O_2 and O_3 classes are the two most abundant chemical classes in all samples except nylon, the profile of which was instead dominated by N_1 classes. The O_2 and O_3 classes also clustered together with the O_1 and O_4 classes, which is in line with the proposal that most

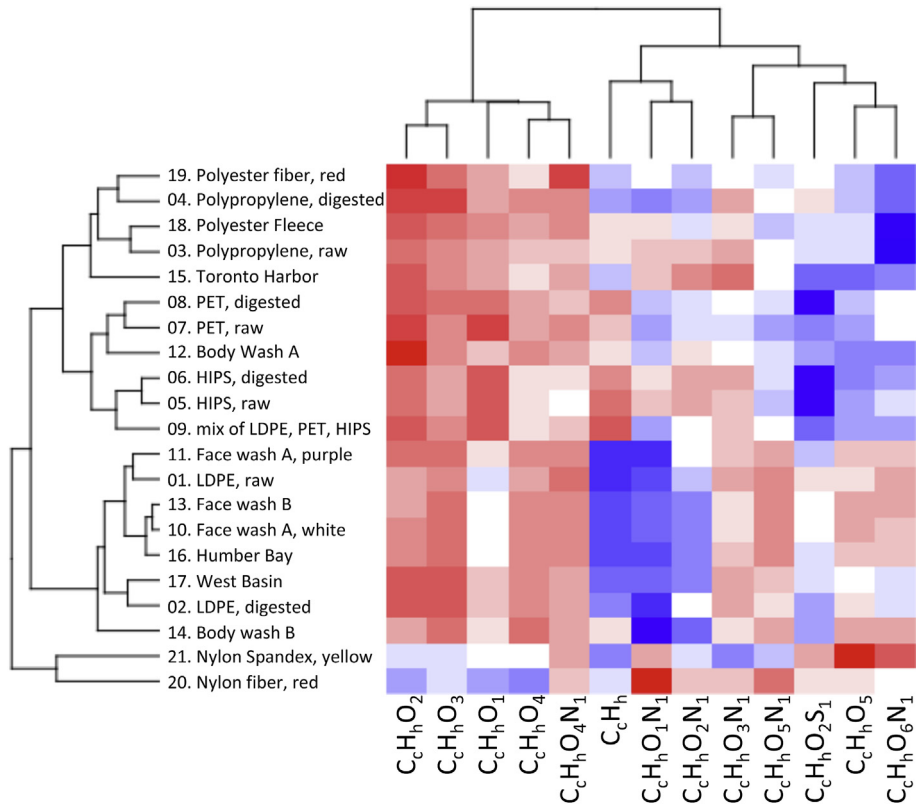


Fig. 6. Hierarchical cluster analysis plot showing relative abundance pyrolysis products sorted by heteroatom content. The red to blue color scale indicates high to low abundance. Elemental composition classes considered in this analysis were present in >50% of the samples.

oxygen compounds are generated by thermooxidation during pyrolysis. The degree of oxidation varied among the different plastics. For example, the relative abundance of hydrocarbon ions (C_cH_n) generated from polyethylene is much lower than from PET or polystyrene. Both PET and polystyrene have structures containing phenyl groups. It may well be that their pyrolysis products retain this aromatic character, which could be less susceptible to reaction with oxygen in ambient air than saturated species.

Nitrogen containing ions were detected as pyrolysis products of all the plastic samples despite the fact that nylon was the only material that contains nitrogen in its structure. Most of the NO_o (where the number of oxygen atom $o = 1, 2, 3, 4$) classes clustered together, which suggests a common mechanism of formation. It has been demonstrated that ammonium adducts can form in ambient air from molecules ionized by positive mode of DART [34,41]. Fig. S1 shows correlation analysis on the intensities between the O_o compounds and their ammoniated counterparts NO_o for the plastic materials analyzed. The strongest correlations ($r = 0.94, p < 0.001$) were found for the polystyrene samples. We can infer that chemicals of O_o classes generated from pyrolysis of polystyrene have proton affinities that are close to that of ammonia. Correlations between $C_cH_nO_o$ and $C_cH_nO_oN_1$ are weaker for polyethylene ($r = 0.83–0.87$) and polypropylene ($r = 0.36–0.67$) but significant. Of the products generated from pyrolysis of polyethylene and polypropylene, those with higher carbon number appear to have greater tendency to form ammonium adducts (Fig. S1). Indeed, it is well known that the proton affinities of alkylated compound increase with carbon number [44]. Correlations between O_o and NO_o for PET are weak and not significant for the processed sample. Such weak correlations suggest that decomposition products with diverse properties are generated from PET. Although the NO_o

compounds are mostly formed during DART ionization instead of from the polymers themselves, their abundances are related to chemical properties such as proton affinity of compounds generated from pyrolysis, which we argue further contributes to the microplastic fingerprint.

3.3. Visualizing and comparing the chemical fingerprints of environmental microplastics

The mass spectra shown in Fig. 2 illustrate that pyrolysis of plastics results in the formation of mixtures of degradation products whose complexity is similar to that of crude oil [30,45–47]. For crude oil, petroleomics approaches have been developed and successfully used to relate chemical compositions to properties and sources of oil, often by visual comparison of graphically sorted elemental compositions. Kendrick mass defect plots and van Krevelen diagrams have proven to be essential in sorting and visualizing the thousands of chemical compositions, usually based on carbon number, double bond equivalents (DBE) and chemical class, i.e. those elemental compositions that share the same number of constituent heteroatoms. Herein, the same visualization approach was employed for analyzing microplastics. The plots obtained from four raw plastic materials analyzed in this study are displayed in Fig. 7 while those for other (environmental) samples are presented in Figs. S2–S4.

Fig. 7A and Fig. S2 display the relative abundance of heteroatom classes generated by pyrolysis of the microplastics. The most abundant classes are $C_cH_nO_o$ (where $o = 2–4$). Nylon (Fig. S2) is the only exception, being different from other polymers due to nitrogen atoms in the structure. For simplicity, Fig. 7A and S2 display N_1 and N_2 classes only. (The number of nitrogen atoms in the observed ions

increases with the size of nylon oligomer). Among all the oxygenated ions, the O₂, O₃ and O₄ classes are the three most abundant for the untreated polyethylene samples and all the samples from personal care products and the environment except sample 14. Principle component analysis had revealed that sample 14 clusters with PET (Fig. 4), and indeed the elevated levels of NO_{5–10} ions (Fig. S2) is consistent with the profile obtained from PET (Fig. 7a). The PET samples (7, 8, 18, 19) all featured elevated NO₄, NO₆ and NO₈ classes. The polystyrene samples showed a higher abundance of hydrocarbon ions (C_cH_h) than other samples.

Van Krevelen plots were generated showing hydrogen-to-carbon (H/C) and oxygen-to-carbon (O/C) ratios, see Fig. 7B and S3. In these plots, homologous elemental compositions fall on a line that crosses the point (O/C = 0, H/C = 2). The lines extend from this origin incrementally by CH₂ units. Hydrocarbon ions (C_cH_h) lie on the vertical line where O/C = 0. The slopes of these lines are determined by the number of oxygen atoms (o) as represented by the equation of H/C = [2 (1-DBE)/o]•(O/C) + 2. In this relationship, only saturated homologues (with DBE = 0 or 0.5) form lines with positive slopes. The slopes decrease to 0 and then negative as the degree of unsaturation increases. Most elemental compositions obtained from polyethylene and polypropylene occupy the upper

regions of van Krevelen plots, whereas the lower left region is mainly occupied by the elemental compositions from polystyrene and PET. These chemicals were primarily highly unsaturated O₁ and O₂ chemical classes. We note that the larger points indicated in Fig. 7B represent trimer and dimer ions [C₂₄H₂₂O + H]⁺ and [C₁₆H₁₄O + H]⁺ from polystyrene and constitute c. 25% of intensity of the O₁ class. Ions [C₉H₈O₂+H]⁺ from PET contributed 27% to the intensity of the O₂ class. The van Krevelen plots obtained from the PET samples display more points occupying the right region (O/C > 0.3) compared to that of polystyrene. This suggests that compounds containing more oxygen atoms are generated from PET, which is consistent with the fact that its monomer contains 4 oxygen atoms.

The carbon number versus DBE plots are displayed in Fig. 7C and S4. Polyethylene and polypropylene primarily occupy the lower region of the plots because their decomposition products are more saturated (with DBEs less than 10 and 7, respectively) than those of polystyrene and PET. Plots for some samples from personal care products (sample 10 and 13) and from the environment (sample 16 and 17) match that for the raw polyethylene. Sample 11 was from the same product as sample 10 but exhibited a lower melting point [33]. Comparing the plots of the two samples, the carbon chain

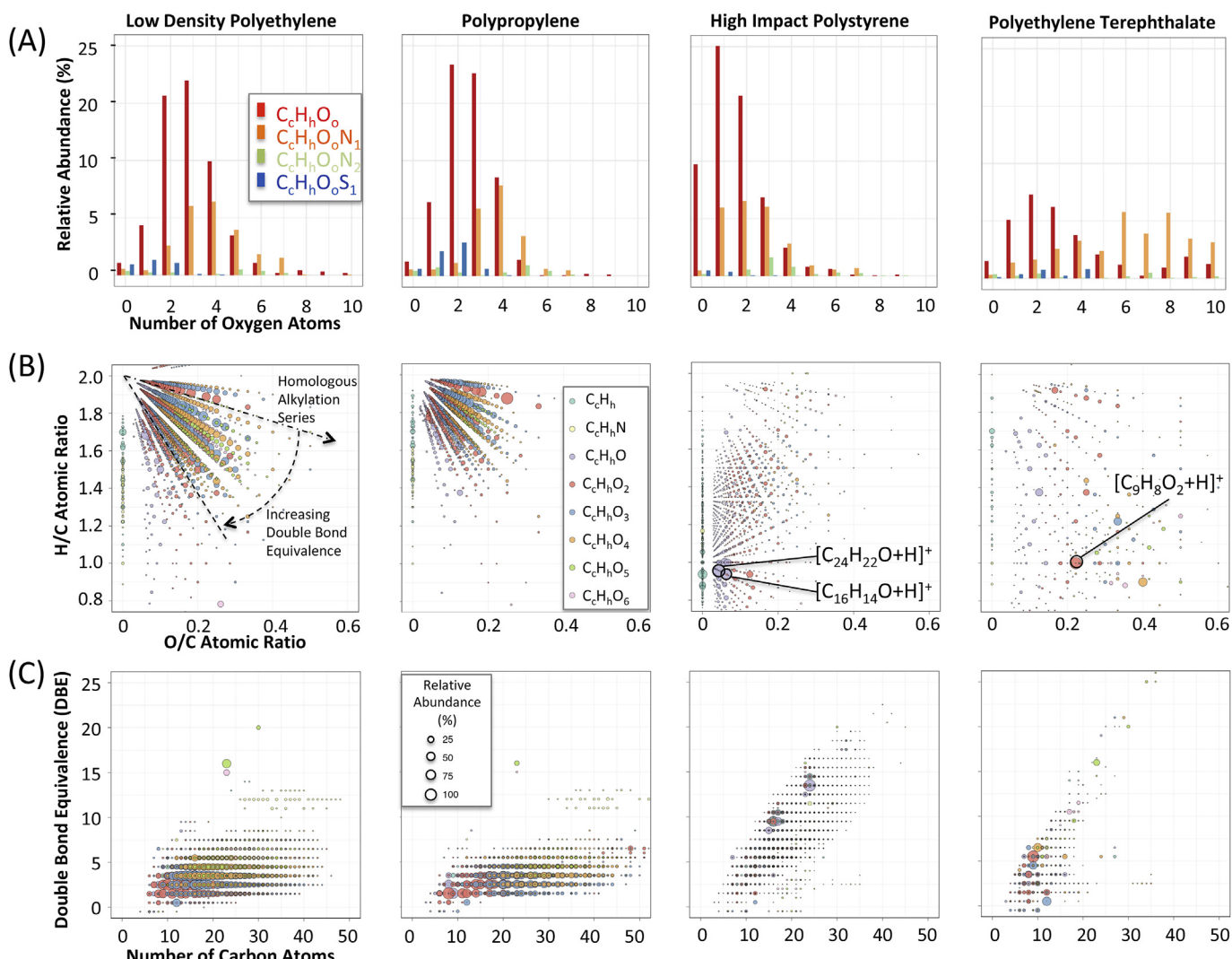


Fig. 7. Differentiation of complex mixtures generated from pyrolysis of untreated ground low-density polyethylene, polypropylene, high impact polystyrene and polyethylene terephthalate using (A) plots of chemical classes distributions, (B) van Krevelen plots and (C) carbon number versus double bond equivalence (DBE) plots.

Table 2

Tentative identifications of plastic additives released from thermal desorption of the microbeads from personal care products and environmental microplastics.

Formula	ID [c]	CAS Number	Type of Additive	Theoretical Mass	Detection in Samples (difference from theoretical mass in ppm/difference from theoretical ^{13}C isotope abundance) Sample Number							
					10	11	12	13	14	15	16	17
[C ₁₈ H ₃₀ O + NH ₄] ⁺	A	17540759	Antioxidant	280.2640 263.2375	-[a]	—	—	—	—	-2.6/-15%	—	—
[C ₁₂ H ₂₂ O ₄ +H] ⁺	B	106796	Plasticizer	231.1596	—	—	-2.3/-12%	—	—	-3.6/-9%	—	—
[C ₁₂ H ₂₇ O ₄ P + H] ⁺	C	126738	Plasticizer	267.1725	—	—	—	—	—	-3.1/7%	—	—
[C ₁₃ H ₁₁ N ₃ O] ⁺	D	2440224	UV Stabilizer	225.0902	—	—	3.1/-13%	2.2/-13%	—	2.6/-7%	—	—
[C ₆ H ₁₄ O ₄] ⁺	E	68186301	Plasticizer	150.0892	—	-4.9/-2%	-4.2/-4%	-4.9/-5%	—	—	—	—
[C ₂₆ H ₅₀ O ₄ +NH ₄] ⁺	F	122623	Plasticizer	444.4053	—	—	—	—	-2.9/-12%	-2.9/4%	—	—
[C ₁₃ H ₁₃ N ₃] ⁺	G	102067	Cross-Linking Agent	211.1109	—	—	—	1.7/-11%	—	2.6/-11%	—	—
[C ₂₄ H ₃₈ O ₄ +H] ⁺	H	117817 [b]	Plasticizer	391.2848	-0.3/-3%	-4.4/10%	-0.9/6%	—	—	-1.9/-3%	-1.1/-1%	-2.1/1%

Notes: [a] ‘—’ indicates no ions in the mass spectra met the criteria when screening against the plastic additive library; [b] Also represented by CAS registry numbers of 6422862 and 27554263; [c] A – 4-(butan-2-yl)-2,6-di-*tert*-butylphenol; B – Decanedioic acid, 1,10-diemethyl ester; C – Tributyl phosphate; D – 2-Benzotriazolyl-4-methylphenol; E – 2,2'-(1,2-ethanediylbis(oxy))bis(ethanol); F – Decanedioic acid, bis(2-ethylhexyl) ester; H – N,N'-diphenyl guanidine; G – Di(2-ethylhexyl) phthalate.

length of the pyrolysis products from sample 11 was shorter in length suggesting the polymer has a lower molecular weight distribution. There were also chemicals with higher DBE generated from sample 11. Sample 12 was similar to sample 11 on these features. At first glance, the plot of sample 15 appears similar to that of PE. However, the abundance of the C_cH_bO₂ ions (see Fig. S4) display a pattern consistent with the presence of PP: ions differing by 42 Da are enhanced in abundance. The similarity of the plot obtained from PET and Sample 14 suggest that this sample consists of PET. These results suggest that relatively simple diagrams (e.g. van Krevelen or C# vs. DBE) may serve to visualize and differentiated the fingerprints of (environmental) microplastics. A library covering variety of samples within each plastic type needs to be built for more generalized plastic classification.

Finally, the use of pyrolysis-HRMS to track sources of pollution of microplastics hinges on a firm understanding of how their chemical fingerprints may change in the environment, due to weathering (e.g. exposure to UV irradiation) and during sample pretreatment. Our experiments reveal very little difference between untreated and digested microplastics by the distribution of elemental composition classes. For example, the distribution of oxygen classes (Fig. S2) do not significantly change despite the use of Fenton's reagent. The only exception is the distribution of ammonium adducted ions NO_o observed in the spectra of LDPE, which fluctuates significantly. However, this may be consequence of lack of control over the ionization reagent (NH₃), which originates from background air in the laboratory.

3.4. Identifying plastic additives released during thermal desorption

Pyrolysis is a destructive technique, but we hypothesize that important information can be gleaned from the profile of chemical additives and other leachable chemicals in environmental microplastics that are detected at lower temperatures. Mass spectra obtained from the virgin plastics, personal care products and environmental samples during the thermal desorption stage (Fig. 1C-II) were screened against a library of plastic additives. Chemicals that met the screening criteria (Section 2.3) are listed in Table 2. Elemental compositions were assigned based on accurate mass and isotope ratios. Subsequent tandem mass spectrometry experiments were not performed. Consequently, we have assigned confidence level 4 to these assignments according to the scheme proposed by Schymanski et al. [51]. The putative additives found in the samples include plasticizers, antioxidants and cross-linking agents. The sample from Toronto Harbor contains more of the identified additives than other samples. We note that the presence of these compounds in the environmental microplastics does not

necessarily mean the additives originate from the plastic. Microplastics may mimic passive sampling devices [14,15,48] and equilibrate with the surrounding environment, including those used as plastic additives. Although such processes would change the additive profiles in the sample, the abundance of additives from absorption will likely be lower than those intentionally added to the material. Uptake of chemicals from a heavily urban impacted area may well explain why the sample from Toronto Harbor contains such a variety of putative additives. On the other hand, the samples from Humber River, another urban impacted site proximal to Toronto Harbor, and the west basin of Lake Erie were comparatively clean. Some plasticizers were tentatively identified in the microbeads from personal care products, which is consistent with a previous survey [49], and included decanedioic acid, 1,10-dimethyl ester or decanedioic acid, bis(2-ethylhexyl) ester. However, these could be residuals from the surfactant materials in the washes. As suggested in Table 2, the profiles of putative additives in the personal care products vary, and such profiles measured during thermal desorption could be useful for source identification, especially when combined with the chemical fingerprint information gained from pyrolysis.

4. Conclusions

In this study, a potentially high throughput analytical method was developed to characterize plastics used in industry, consumer products and sampled from the environment, using thermal desorption and pyrolysis coupled with DART-FTMS. These experiments reveal the rich chemical fingerprints of common environmental microplastics: the complex mixture of polymer degradation products generated by thermal desorption and pyrolysis and reflect the polymer composition as well as presence of additive chemicals. When analyzed by multivariate statistics and visualized by Kendrick mass defect and van Krevelen diagrams, these chemical fingerprints provide diagnostic information on the composition of the polymer and its additives. This information can potentially link the occurrence and sources of environmental microplastics, akin to how similar approaches have been used to identify sources of petroleum spills [46]. Such information would aid in the development and prioritization of management actions to reduce the emission of microplastics to the environment.

Pyrolysis GC-MS is rapidly gaining popularity and may well become the *de facto* method for both qualitative and quantitative analysis of micro- and nanoplastics that are beyond the detection limits and spatial resolution of spectroscopic techniques. Apart from differences that may arise due to the residence time in the GC column, it is expected that the compounds detected by DART-FTMS

will closely match those measured by pyrolysis GC-MS. This study underlines the fact that highly complex mixtures of chemicals are generated during pyrolysis that cannot be distinguished by low-resolution MS alone. Few studies to date have published identities on more than a handful of signature compounds and some of the more convincing attempts at quantitation [39] have not been reproduced. Reliable quantitative measurements of microplastics and nanoplastics will require the firm identification of target compounds, potential interferences and the synthesis of authentic (isotopically labelled) standards [50].

Author contribution

Xianming Zhang: Conceptualization, Methodology, Writing – Original Draft, Review and Editing; **Alicia Mell:** Data curation, Methodology **Frederick Li:** Data curation, Methodology **Clara Thaysen:** Writing – Original Draft **Brian Musselman:** Resources, Validation **Joseph Tice:** Resources; **Dragan Vukovic:** Resources, Validation; **Chelsea Rochman:** Resources, Validation, **Paul A. Helm:** Conceptualization, Resources, Validation **Karl J. Jobst:** Conceptualization, Project administration.

Declaration of competing interest

The authors declare that they have no known competing financial interests or personal relationships that could have appeared to influence the work reported in this paper.

Acknowledgments

We acknowledge the students and staff of the Great Lakes unit for collection and preparation of environmental and personal care samples. KJJ thanks Dr. Vince Taguchi for introducing him to the art of DART. Thanks to the Herbert W Hoover Foundation for funding C Thaysen during this work.

Appendix A. Supplementary data

Supplementary data to this article can be found online at <https://doi.org/10.1016/j.aca.2019.12.005>.

References

- [1] Plastics Europe, Plastics – the Facts. https://www.plasticseurope.org/application/files/5715/1717/4180/Plastics_the_facts_2017_FINAL_for_website_one_page.pdf, 2017 accessed Apr 2018.
- [2] R. Geyer, J.R. Jambeck, K.L. Law, Production, use, and fate of all plastics ever made, *Sci. Adv.* 3 (2017), e1700782.
- [3] K. Duis, A. Coors, Microplastics in the aquatic and terrestrial environment: sources (with a specific focus on personal care products), fate and effects, *Environ. Sci. Eur.* 28 (2016) 2.
- [4] A.A. Horton, A. Walton, D.J. Spurgeon, E. Lahive, C. Svendsen, Microplastics in freshwater and terrestrial environments: evaluating the current understanding to identify the knowledge gaps and future research priorities, *Sci. Total Environ.* 586 (2017) 127–141.
- [5] A. Cázar, F. Echevarría, J.I. González-Gordillo, X. Irigoien, B. Úbeda, S. Hernández-León, Á.T. Palma, S. Navarro, J. García-de-Lomas, A. Ruiz, Plastic debris in the open ocean, *Proc. Natl. Acad. Sci.* 111 (2014) 10239–10244.
- [6] D. Eerkes-Medrano, R.C. Thompson, D.C. Aldridge, Microplastics in freshwater systems: a review of the emerging threats, identification of knowledge gaps and prioritisation of research needs, *Water Res.* 75 (2015) 63–82.
- [7] A.G.J. Driedger, H.H. Dürr, K. Mitchell, P. Van Cappellen, Plastic debris in the Laurentian Great Lakes: a review, *J. Gt. Lakes Res.* 41 (2015) 9–19.
- [8] M. Cole, P. Lindeque, C. Halsband, T.S. Galloway, Microplastics as contaminants in the marine environment: a review, *Mar. Pollut. Bull.* 62 (2011) 2588–2597.
- [9] C.M. Rochman, M.A. Browne, A.J. Underwood, J.A. van Franeker, R.C. Thompson, L.A. Amaral-Zettler, The ecological impacts of marine debris: unraveling the demonstrated evidence from what is perceived, *Ecology* 97 (2016) 302–312.
- [10] C.J. Foley, Z.S. Feiner, T.D. Malinich, T.O. Hook, A meta-analysis of the effects of exposure to microplastics on fish and aquatic invertebrates, *Sci. Total Environ.* 631–632 (2018) 550–559.
- [11] D. Lithner, A. Larsson, G. Dave, Environmental and health hazard ranking and assessment of plastic polymers based on chemical composition, *Sci. Total Environ.* 409 (2011) 3309–3324.
- [12] J.D. Meeker, P.I. Johnson, D. Camann, R. Hauser, Polybrominated diphenyl ether (PBDE) concentrations in house dust are related to hormone levels in men, *Sci. Total Environ.* 407 (2009) 3425–3429.
- [13] M. Manikkam, R. Tracey, C. Guerrero-Bosagna, M.K. Skinner, Plastics derived endocrine disruptors (BPA, DEHP and DBP) induce epigenetic transgenerational inheritance of obesity, reproductive disease and sperm epimutations, *PLoS One* 8 (2013), e55387.
- [14] C.M. Rochman, M.A. Browne, B.S. Halpern, B.T. Hentschel, E. Hoh, H.K. Karapanagioti, L.M. Rios-Mendoza, H. Takada, S. Teh, R.C. Thompson, Classify plastic waste as hazardous, *Nature* 494 (2013a) 169.
- [15] C.M. Rochman, E. Hoh, B.T. Hentschel, S. Kaye, Long-term field measurement of sorption of organic contaminants to five types of plastic pellets: implications for plastic marine debris, *Environ. Sci. Technol.* 47 (2013b) 1646–1654.
- [16] T. Rocha-Santos, A.C. Duarte, A critical overview of the analytical approaches to the occurrence, the fate and the behaviour of microplastics in the environment, *TrAC Trends Anal. Chem.* (Reference Ed.) 65 (2015) 47–53.
- [17] V. Hidalgo-Ruz, L. Gutow, R.C. Thompson, M. Thiel, Microplastics in the marine environment: a review of the methods used for identification and quantification, *ES T (Environ. Sci. Technol.)* 46 (2012) 3075.
- [18] M.A. Browne, P. Crump, S.J. Niven, E. Teuten, A. Tonkin, T. Galloway, R. Thompson, Accumulation of microplastic on shorelines worldwide: sources and sinks, *Environ. Sci. Technol.* 45 (2011) 9175–9179.
- [19] P.A. Helm, Improving microplastics source apportionment: a role for microplastic morphology and taxonomy? *Analytical Methods* 9 (2017) 1328–1331.
- [20] W.J. Shim, S.H. Hong, S.E. Eo, Identification methods in microplastic analysis: a review, *Analytical Methods* 9 (2017) 1384–1391.
- [21] Y.K. Song, S.H. Hong, M. Jang, G.M. Han, M. Rani, J. Lee, W.J. Shim, A comparison of microscopic and spectroscopic identification methods for analysis of microplastics in environmental samples, *Mar. Pollut. Bull.* 93 (2015) 202–209.
- [22] A. Käppeler, D. Fischer, S. Oberbeckmann, G. Schernewski, M. Labrenz, K.-J. Eichhorn, B. Voit, Analysis of environmental microplastics by vibrational microscopy: FTIR, Raman or both? *Anal. Bioanal. Chem.* 408 (2016) 8377–8391.
- [23] Z. Sobhani, M. Al Amin, R. Naidu, M. Megharaj, C. Fang, Identification and visualisation of microplastics by Raman mapping, *Anal. Chim. Acta* 1077 (2019) 191–199.
- [24] E. Fries, J.H. Dekiff, J. Willmeyer, M.-T. Nuelle, M. Ebert, D. Remy, Identification of polymer types and additives in marine microplastic particles using pyrolysis-GC/MS and scanning electron microscopy, *Environ. Sci.: Processes & Impacts* 15 (2013) 1949–1956.
- [25] E. Dümichen, P. Eisentraut, C.G. Bannick, A.-K. Barthel, R. Senz, U. Braun, Fast identification of microplastics in complex environmental samples by a thermal degradation method, *Chemosphere* 174 (2017) 572–584.
- [26] M. Fischer, B.M. Scholz-Bottcher, Simultaneous trace identification and quantification of common types of microplastics in environmental samples by pyrolysis-gas chromatography-mass spectrometry, *Environ. Sci. Technol.* 51 (2017) 5052–5060.
- [27] A. Ter Halle, L. Jeanneau, M. Martignac, E. Jarde, B. Pedrono, L. Brach, J. Gigault, Nanoplastic in the North Atlantic subtropical Gyre, *Environ. Sci. Technol.* 51 (2017) 13689–13697.
- [28] L. Hermabessiere, C. Himber, B. Boricaud, M. Kazour, R. Amara, A.-L. Cassone, M. Laurentie, I. Paul-Pont, P. Soudant, A. Dehaut, G. Duflos, Optimization, performance, and application of a pyrolysis-GC/MS method for the identification of microplastics, *Anal. Bioanal. Chem.* 410 (2018) 6663–6676.
- [29] X-x Zhou, L-t Hao, H. Wang, Y. Li, J. Liu, 1-Cloud-Point extraction combined with thermal degradation for nanoplastic analysis using pyrolysis gas chromatography–mass spectrometry, *Anal. Chem.* 91 (2019) 1785–1790.
- [30] A.G. Marshall, R.P. Rodgers, Petroleomics: the next grand challenge for chemical analysis, *Acc. Chem. Res.* 37 (2004) 53–59.
- [31] L.K. Ackerman, G.O. Noonan, T.H. Begley, Assessing direct analysis in real-time-mass spectrometry (DART-MS) for the rapid identification of additives in food packaging, *Food Addit. Contam. Part A Chem. Anal. Control Expo Risk Assess* 26 (2009) 1611–1618.
- [32] M. Haunschmidt, C.W. Klampfl, W. Buchberger, R. Hertsens, Rapid identification of stabilisers in polypropylene using time-of-flight mass spectrometry and DART as ion source, *Analyst* 135 (2010) 80–85.
- [33] K. Munno, P.A. Helm, D.A. Jackson, C. Rochman, A. Sims, Impacts of temperature and selected chemical digestion methods on microplastic particles, *Environ. Toxicol. Chem.* 37 (2018) 91–98.
- [34] J.H. Gross, Direct analysis in real time—a critical review on DART-MS, *Anal. Bioanal. Chem.* 406 (2014) 63–80.
- [35] M. Loos, C. Gerber, F. Corona, J. Hollender, H. Singer, Accelerated isotope fine structure calculation using pruned transition trees, *Anal. Chem.* 87 (2015) 5738–5744.
- [36] M. Bolgar, J. Hubball, J. Groeger, S. Meronek, *Handbook for the Chemical Analysis of Plastic and Polymer Additives*, CRC Press, 2007.
- [37] T. Kind, O. Fiehn, Seven Golden Rules for heuristic filtering of molecular formulas obtained by accurate mass spectrometry, *BMC Bioinf.* 8 (2007) 105.
- [38] W. Kew, J.W. Blackburn, D.J. Clarke, D. Uhrin, Interactive van Krevelen diagrams—Advanced visualisation of mass spectrometry data of complex

- mixtures, *Rapid Commun. Mass Spectrom.* 31 (2017) 658–662.
- [39] G. Montaudo, C. Puglisi, F. Samperi, Primary thermal degradation mechanisms of PET and PBT, *Polym. Degrad. Stab.* 42 (1993) 13–28.
- [40] R.E. Adams, Positive and negative chemical ionization pyrolysis mass spectrometry of polymers, *Anal. Chem.* 55 (1983) 414–416.
- [41] N. Sugimura, A. Furuya, T. Yatsu, T. Shibue, formation of ammonium ion adduct molecules in positive direct analysis in real time (DART) ionization mass spectrometry, *J. Mass Spectrom. Soc. Jpn.* 62 (2014) 25.
- [42] P. Punnarak, S. Tantayanon, V. Tangpasuthadol, Dynamic vulcanization of reclaimed tire rubber and high density polyethylene blends, *Polym. Degrad. Stab.* 91 (2006) 3456.
- [43] A.B. Silva, A.S. Bastos, C.I.L. Justino, J.P. da Costa, A.C. Duarte, T.A.P. Rocha-Santos, Microplastics in the environment: challenges in analytical chemistry – a review, *Anal. Chim. Acta* 1017 (2018) 1–19.
- [44] J. Evans, G. Nicol, B. Munson, Proton affinities of saturated aliphatic methyl esters, *J. Am. Soc. Mass Spectrom.* 11 (2000) 789–796.
- [45] R.P. Rodgers, T.M. Schaub, A.G. Marshall, *Petroleumics: MS Returns to its Roots*, ACS Publications, 2005.
- [46] A.G. Marshall, R.P. Rodgers, *Petroleumics: chemistry of the underworld*, Proc. Natl. Acad. Sci. 105 (2008) 18090–18095.
- [47] C.S. Hsu, C.L. Hendrickson, R.P. Rodgers, A.M. McKenna, A.G. Marshall, Petroleumics: advanced molecular probe for petroleum heavy ends, *J. Mass Spectrom.* 46 (2011) 337–343.
- [48] Y. Ogata, H. Takada, K. Mizukawa, H. Hirai, S. Iwasa, S. Endo, Y. Mato, M. Saha, K. Okuda, A. Nakashima, M. Murakami, N. Zurcher, R. Booyatumanondo, M.P. Zakaria, L.Q. Dung, M. Gordon, C. Miguez, S. Suzuki, C. Moore, H.K. Karapanagioti, S. Weerts, T. McClurg, E. Burres, W. Smith, M. Van Velkenburg, J.S. Lang, R.C. Lang, D. Laursen, B. Danner, N. Stewardson, R.C. Thompson, International Pellet Watch: global monitoring of persistent organic pollutants (POPs) in coastal waters. 1. Initial phase data on PCBs, DDTs, and HCHs, *Mar. Pollut. Bull.* 58 (2009) 1437–1446.
- [49] J.C. Hubinger, A survey of phthalate esters in consumer cosmetic products, *J. Cosmet. Sci.* 61 (2010) 457–465.
- [50] M. Sander, H.-P. Kohler, K. McNeill, Assessing the Environmental Transformation of Nanoplastics through ^{13}C -Labelled Polymers, vol. 14, 2019, pp. 301–303.
- [51] E.L. Schymanksi, J. Jeon, R. Gulde, K. Fenner, M. Ruff, H.P. Singer, J. Hollender, *ES&T*, 2014, 48, 2097–2098.

Rapid fingerprinting of source and environmental microplastics using Direct analysis in real time-high resolution mass spectrometry

Xianming Zhang^{1,*}; Alicia Mell¹; Frederick Li²; Clara Thaysen³; Brian Musselman²;

Joseph Tice²; Dragan Vukovic⁴; Chelsea Rochman³; Paul A. Helm¹; Karl J. Jobst^{1,5*}

1. Ontario Ministry of the Environment, Conservation and Parks, Toronto, Ontario M9P 3V6, Canada

2. IonSense Inc. Saugus, Massachusetts 01906, USA

3. Department of Ecology and Evolutionary Biology, University of Toronto, Toronto, Ontario M5S 3H6, Canada

4. VBM Science Ltd., Dundas, Ontario L9H 6Y7, Canada

5. Department of Chemistry, Memorial University of Newfoundland, St. John's, NL A1B 3X7, Canada (current address)

*Corresponding authors: xianming.zhang@gmail.com; kjobst@mun.ca

Supplementary Material

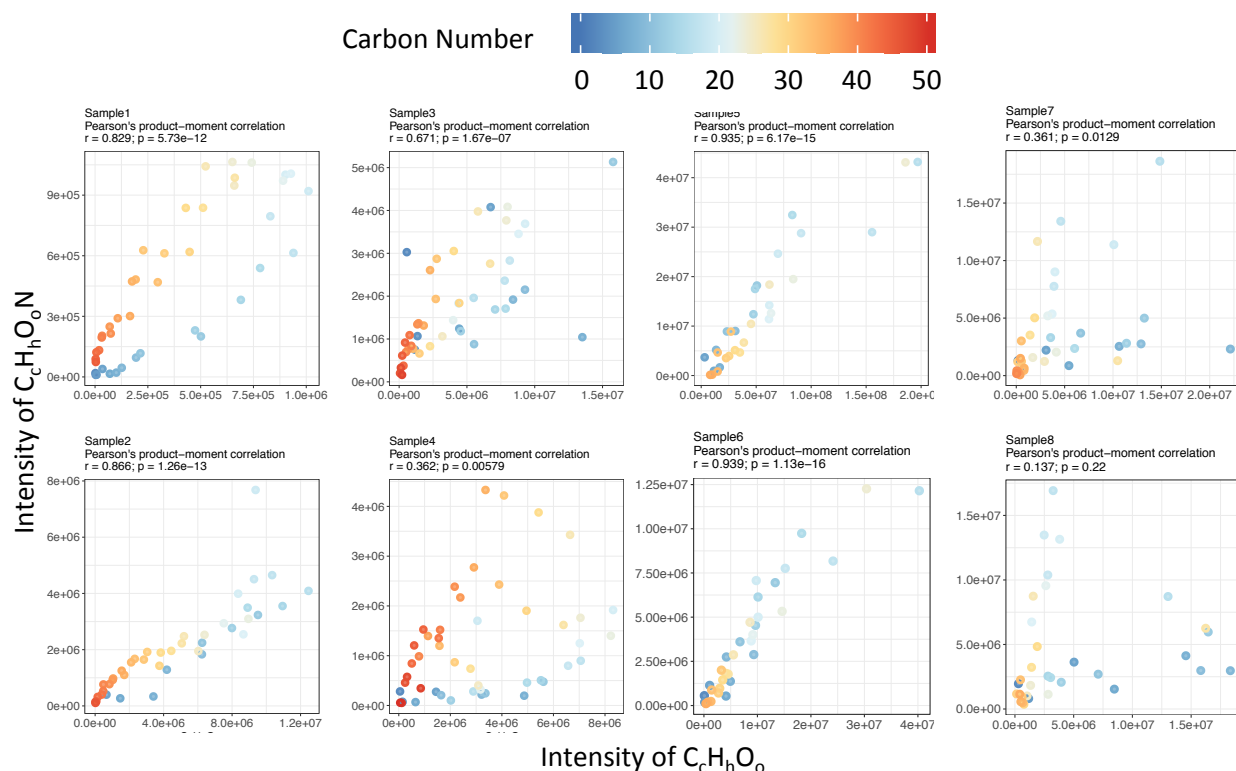


Figure S1. Relationship between intensities of $C_cH_hO_o$ and $C_cH_hO_oN_1$ classes for the untreated (samples 1,3,5,7) and digested plastic materials (samples 2,4,6,8). The degree of ammoniation increases in the polyolefin samples (1,2,3,4) as the carbon chain and proton affinity increases.

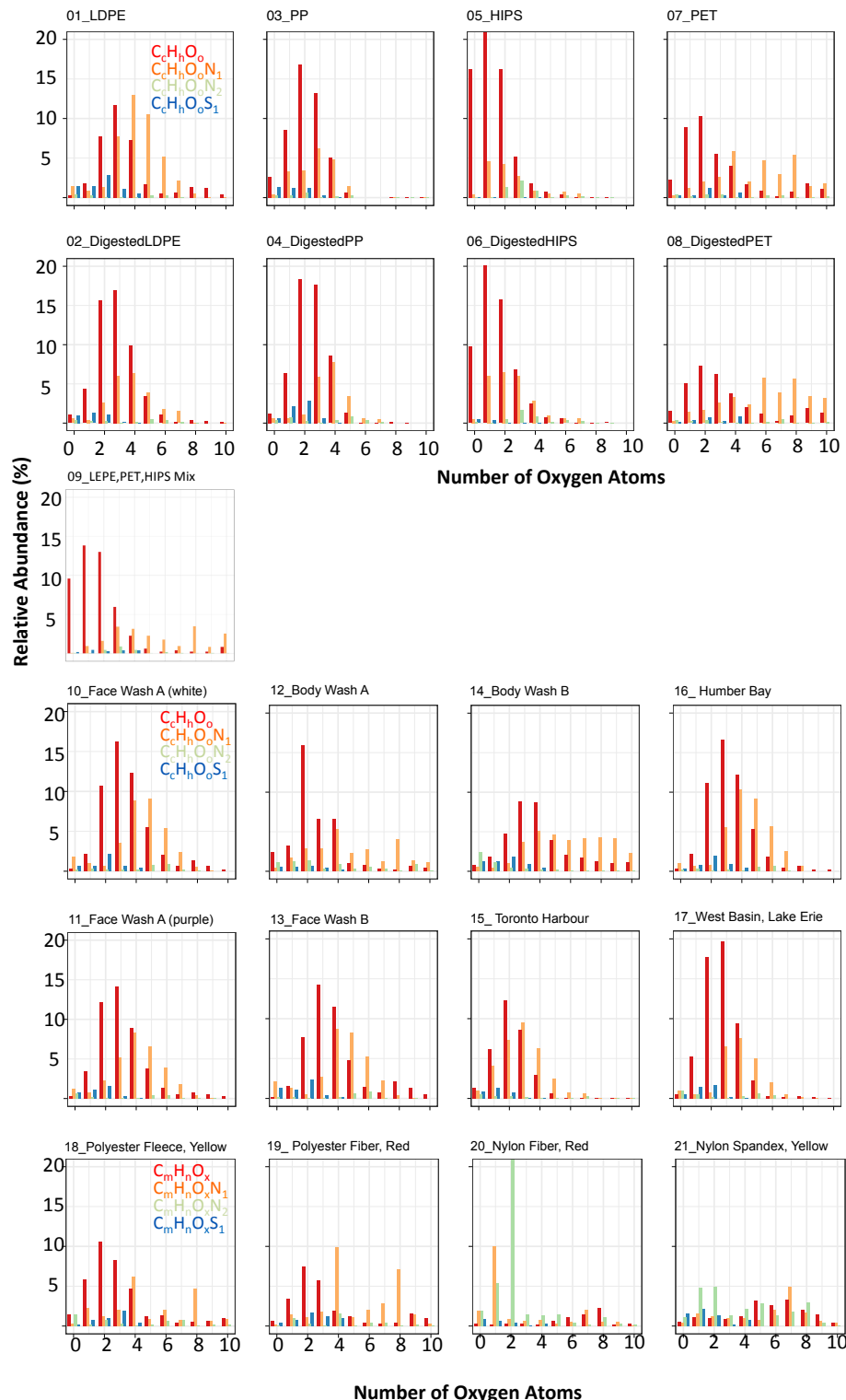


Figure S2. Visualization of complex mixtures generated from pyrolysis of the plastic samples using plots of chemical classes distributions.

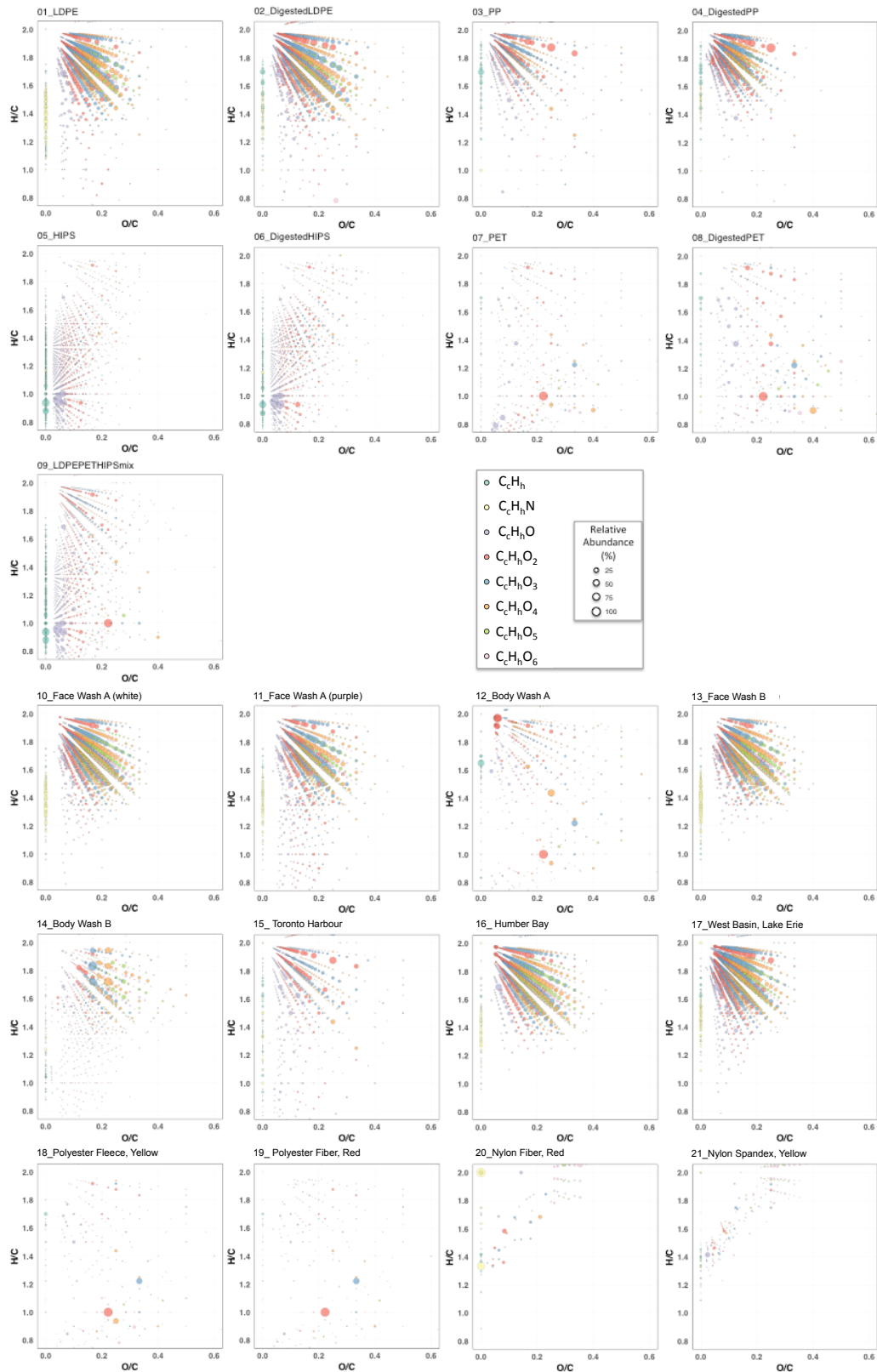


Figure S3. Visualization of complex mixtures generated from pyrolysis of the plastic samples using van Krevelen plots.

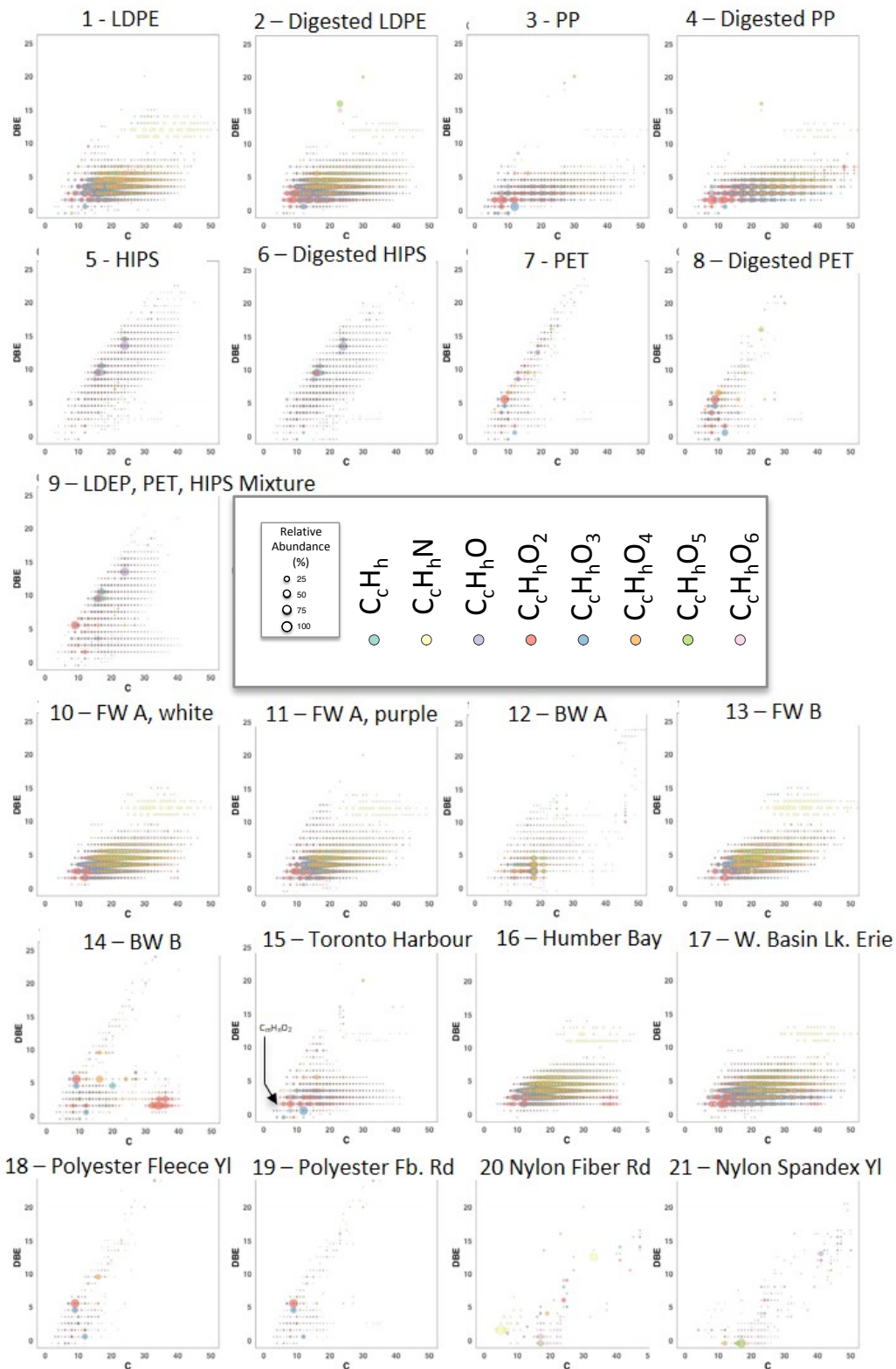


Figure S4. Visualization of complex mixtures generated from pyrolysis of the plastic samples using carbon number versus double bond equivalence (DBE) plots.